Hybrid Deep Learning Algorithm for the State of Charge Prediction of the Lithium-Ion Battery for Electric Vehicles

Sugashini, Rajarathinam; Mangaiyarkarasi, Soundarrajan Padmanadhan[*+]
Department of Electrical and Electronics Engineering, University College of Engineering, Panruti-607106, Tamilnadu, INDIA

ABSTRACT: *An accurate and dependable evaluation of the State of Charge (SOC) is required to maximize battery life and safety. The primary goals of this research are to identify dual-polarization parameters and estimate SOC. Dynamic identification of model parameters and estimation of battery SOC are achieved by co-estimating recursive Chicken Swarm Optimization (CSO) and Grey Wolf Optimization (GWO) algorithms from real-time current and voltage measurement data. A dual-polarization model's projected voltage is nearly the same as the actual voltage to better depict the dynamic properties of the battery and the identification process. Adaptive noise variance updating techniques applied to the extended improve SOC estimates. As a result, the proposed technique is validated using Dynamic Stress Test (DST) data and a Federal Urban Driving Schedule (FUDS). During FUDS testing, an estimated error of less than 2% and a root-mean-square error of less than 0.01085 are observed. We discovered that the approach can withstand erroneous beginning SOCs and other measurement noise covariance in the robustness study.*

KEYWORDS: *Electric vehicle; LSTM; CSO; GWO; Battery management system*

INTRODUCTION

Electric vehicles are now the primary mode of transportation because they are both environmentally and economically friendly [1]. The battery management system is a critical component of Electric Vehicles (EVs). Lithium-Ion Batteries (LIB) have become the most important component of EVs due to their high energy density and long service life. The State of Charge (SoC) of the Battery Management System (BMS) is a critical metric. Correct assessment can ensure charge/discharge safety and alleviate range anxiety in EVs. However, because LIB is a nonlinear, time-varying system, directly measuring SoC is difficult, making its estimation a difficult task for BMS [2].

Batteries, unlike fossil fuels, require precise monitoring to improve performance, extend life, and improve battery management, particularly with large-scale battery packs. *Vellingiri et al* propose the LSTM hybrid convolution neural network in their studies to improve the performance of the renewable energy system for hybrid electric vehicles. [3] That the SoC has a direct impact on the

******To whom correspondence should be addressed.*
+ *E-mail: rsugashini01@gmail.com*
1021-9986/2023/8/2650-2660 11/$/6.01

available battery capacity [4]. The range of a device is directly related to its battery capacity, and indirectly to its battery capacity. Sensors cannot detect SoC directly to avoid interference from the electrochemical process. As a result, estimation techniques based on observable parameters such as current or terminal voltage are needed to calculate its value. Because of their importance in terms of improving performance and battery life, the Battery Management System (BMS) and estimation of battery metrics such as SoC and SoH have been the focus of much recent research [5]. Real-time monitoring of battery utilisation necessitates the use of an efficient Battery Management System (BMS), which evaluates the battery state to ensure safe operation. In the literature, there are several approaches to building a BMS. The charge status of a BMS is an important factor in its performance. It is critical to accurately estimate the SoC in order to increase battery cycle life, improve energy management, reduce costs, and ensure the overall safety of the PV system. Because of the storage battery's nonlinear properties and intricate electrochemical interactions, obtaining an accurate online calculation of SoC is difficult. The SoC (state of charge) is a measurement of the remaining capacity of the battery. It is the ratio of a capacity's actual value to its notional value. There are several methods for estimating the SoC, each with advantages and disadvantages. Traditional methods, such as Coulomb counting, have been used because they are simple. This method has several flaws, including the accumulation of current measurement errors caused by disturbances and the requirement of prior knowledge of starting values for accurate results. Much effort has been expended in recent years to improve the accuracy of SoC estimations.

Popular methods for calculating SoC include Ampere-hour (Ah) counting and impedance testing [6, 7]. Their simplicity, low cost, and user-friendliness make them appealing, but their inaccuracy cannot be denied due to the sum of individual measurement mistakes that occur during integration. Temperature and time are additional factors when measuring impedance. Estimating the SoC may be done with the use of several AI methods, such as Adaptive Neuro-Fuzzy Inference Systems (ANFIS), Neural Networks (NN) [9-11], Fuzzy Inference Systems (FIS) [12,13], and Learning-Based Algorithms (LbAs). These methods are accurate enough to use in practise without resorting to an overly exact battery model. Thus, the system is treated as a black box, and its state variables are calculated by looking at historical data. However, NN-based solutions need a lot of trustworthy training data and powerful technological hardware. It is common practise to utilise a supplementary algorithm, such an optimization method, in tandem with a fuzzy-based algorithm, such as one based on fuzzy sets of rules or membership functions, to increase its effectiveness.

Plett invented the bar-delta filtering method in 2009 to calculate the SoC of each battery cell as well as the average SoC of the battery pack. In reference, a two-time-scale Extended Kalman Filter (EKF) was used to estimate the pack's average SOC by comparing the SOC of individual cells to that of the "average battery" represented by a simulated circuit. If we use *Plett* and *Dai*'s bar-delta filtering method to estimate the state parameters of each cell, the BMS will still have hundreds of delta filters running at any given time. In reference [16], passive equilibrium control for series battery packs was developed at the cell and module levels, and this was then used to create a multi-scale state estimation architecture based on the pack's "weakest cell." The SoC can be determined using the lowest voltage in the battery pack.

To estimate battery pack SoC [17], a lumped parameter equivalent circuit model was developed that takes into account the inconsistencies between individual battery cells. AEKF was then used to estimate the SoC for the battery pack. *Sun et al*. developed an updated model of a battery pack that takes into account the fact that each of the many cells contains an element of uncertainty. To identify the nominal battery model, average capacity and average resistance are used as filters [18-20] Discovered a direct connection between the first overcharged and first over-discharged cells in a battery pack, which was used to calculate the state of charge of the battery pack. The battery is safe to use, but if this method is used, the State of Charge (SoC) of the battery pack may fluctuate during charging and draining [21]. Zheng and colleagues used a genetic algorithm to determine the best parameters for the equivalent circuit model; the total battery pack SoC was then calculated using a set of rules and thresholds derived from the AEKF method for estimating cell SoC. To calculate the SoC of each battery cell, this method requires time-consuming and complex AEKF matrix transformations. Those who built a Gaussian process regression prediction model and used an efficient feature selection strategy saw their SoC estimates improve even more [22]. The lengthy calculation time of this method is a significant disadvantage. The neural network proposed in [23] considers the terminal current, voltage, state of charge, and surface temperature of the battery to predict the anode potential. Simulated data generated by a pseudo-2D model with empirical validation and a two-state thermal model were used to train the model. Furthermore, [24] compared the precision and space requirements of three different NE potential estimation strategies. A Pseudo-2D model was used to generate test data in order to train a model. It is not necessary to study electrochemistry in depth or to spend a significant amount of time tweaking parameters in the model, as suggested by the data. A large amount of data is frequently required for successful model training. For example, a high-performance computer cluster across the country was used to train a neural network model. The NE potential estimate in these studies [23, 24] is not validated by experimental data, which is a disadvantage.

Because a fractional-order model of the lithium-ion battery may provide a more accurate SOC estimate, a fractional-order adaptive EKF method based on the fractional-order model was developed [25]. An adaptive evolutionary algorithm was used to find the model parameters offline using the fractional-order model and the suggested double EKF estimate approach for lithium-ion batteries [26]. An adaptive fractional-order EKF was implemented using a variance updating method to speed up convergence and increase the robustness of SoC estimation [27]. The use of a fractional-order model to characterise the dynamic properties of lithium-ion batteries is now the dominant approach of SOC calculation based on Kalman filters [28,2 9].

According to research, the state of charge prediction of the battery management system is critical in electric vehicles. For the prediction of the SoC of the BMS system, various algorithms are used [3]. The convolution neural network combined with the LSTM is used in the reference [3]. Convolution neural networks are better suited to image processing data. All of the dataset values in this work are time series. The grey wolf algorithm and a hybrid deep learning algorithm are used in this study for chicken swarm optimization. The BMS system will benefit from the hybrid deep learning algorithm for SoC prediction.

METHODOLOGY

Modelling lithium-ion battery

The dynamic properties of a battery can only be accurately described if a simple and reliable model structure for the battery is developed. A first-order Resistor-Capacitor (RC) model is the best option in terms of accuracy, robustness, and complexity. The RC model is made up of VOC, the internal resistance R0, and one RC parallel capacitance-resistance. I represents the load current, and V represents the terminal voltage of the battery. This is known as the Voltage of Open Circuit (VOC). The ohmic resistance R0 is used to measure the flow of electricity between electrodes, the separator, and the electrolyte. The charge transfer resistance and double-layer capacitance between the electrolyte and the electrode are represented by R_1 and C_1. I_1 is the mathematical representation of R1's current. The voltages V1 and V0 represent the resistor-capacitor RC connection and R0, respectively.

$$V(t) = V_{oc} - R_1 I_1 - R_o I \tag{1}$$

$$I_1 = \frac{1}{R_1 C_1}(I - I_1) \tag{2}$$

$$V_1 = \frac{1}{R_1 C_1} V_1 + \frac{1}{C_1} I \tag{3}$$

Battery test procedure

The dynamic properties of a battery can only be accurately described if a simple and reliable model structure for the battery is developed. A first-order Resistor-Capacitor (RC) model is the best option in terms of accuracy, robustness, and complexity. The RC model is made up of VOC, the internal resistance R0, and one RC parallel capacitance-resistance. I represents the load current, and V represents the terminal voltage of the battery. This is known as the Voltage of Open Circuit (VOC). The ohmic resistance R0 is used to measure the flow of electricity between electrodes, the separator, and the electrolyte. The charge transfer resistance and double-layer capacitance between the electrolyte and the electrode are represented by R1 and C1. I1 is the mathematical representation of R1's current. The voltages V1 and V0 represent the resistor-capacitor RC connection and R0, respectively.

Dataset description

The dataset is obtained from the work of [1] Electric vehicles of the future, hybrid electric vehicles, smart grids, and microgrids all need electrochemical Energy Storage

Table 1: Dataset for the Road condition

Cycle	Training	Testing
Cycle 1	ARB 1640s	Rest 600s
Cycle 2	Rest 1200s	FTP 2478s
Cycle 3	Rep 1401s	SC03 601s
Cycle 4	Rest 1200s	UDDSHDV 1061s
Cycle 5	US06 601s	Rest 1800s
Cycle 6	SC03 601s	REP05 1401s
Cycle 7	Rest 1200s	SC03 601s
Cycle 8	HWFET 766s	UDDS 1370s
Cycle 9	Rest 1200s	Rest 600s
Cycle 10	UDDS 1370s	Constant 1800s
Cycle 11	Rest 1200s	Rest 1800s
Cycle 12	OCC 1910s	UNIF01 1931s
Cycle 13	Rest 1200s	FTP 2478s
Cycle 14	HWFET_MNT 766s	HWFET 766s
Cycle 15	Rest 1200s	OCC 1910s
Cycle 16	Charging	NYCC 599s
Cycle 17	Rest 1200s	Rest 3600s
Cycle 18	VEIL2NREL 5915s	
Cycle 19	Rest 1200s	

Systems to be used effectively (ESSs). Additionally, BMSs are essential for monitoring, maintaining, and even regulating the battery pack itself. A BMS must be able to determine the state of charge of the ESS cells. Most promising are model-based approaches, such as extended or unscented Kalman filters. First, the models must give helpful insights into cell physics to expose specifics of the SoC; second, they must approximate all nonlinear interactions between important physical parameters and provide the most flexibility in defining the system. In addition, this property eliminates the need for time-consuming and specialized tests when fine-tuning the model. So that novel models and associated system identification methods may be tested and evaluated, the data set includes a wide and realistic application of electrochemical cells. Self-created and programmed battery cyclers have been used to gather the data set autonomously, mimicking the functioning of electrochemical cells in an electric vehicle. These results were obtained using a battery pack similar to that seen in Nissan's Leaf electric vehicle, which was powered by a lithium polymer cell model ePLB C020. The particular cell had an effective capacity of 15 Ah, which was relevant to the acquisition endeavor. It is planned to construct the Training and

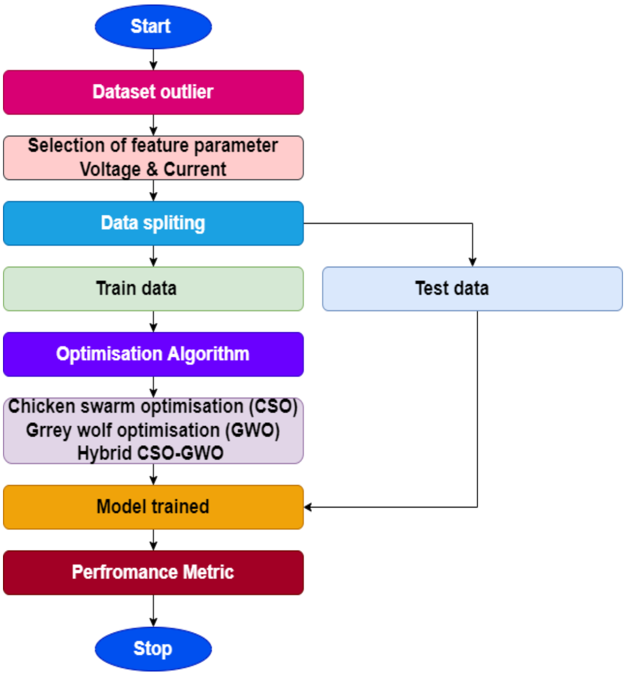

Fig. 1: Methodology adopted in the study

Testing Sets in two trips. Both itineraries were meant to reflect a realistic driving situation by including urban, extra-urban, and highway driving cycles, as well as rests and battery charging intervals. Drive cycles from the Federal Test Procedure repository have been chosen to approximate a typical cell's use. Data from a 277.64-kilometer voyage and a 163.24-kilometer excursion, totalling roughly 12 hours, are used for training and testing, respectively. It was possible to examine the SoC sequence with a one-second sampling interval by using the Coulomb counting approach. The battery pack data analysed in this research include the New European Driving Cycle (NEDC), Federal Urban Driving Schedule (FUDS), the Dynamic Stress Test (DST), and the Urban Dynamometer Driving Schedule (UDDS). During each driving cycle, some measures are taken on the battery pack. These contain measurements of the battery pack's total voltage and trunk current, as well as its discharge capacity and the energy it has been able to discharge. It's a huge amount of data that the battery pack gathers. The data regarding the road condition is shown in Table 1. Using battery voltage models to determine SoC is currently the most used method. Batteries When it comes to electrical voltage modeling, SoC is often seen as a model that specifies the parameters [17]. It is common to characterize OCV as a monotonic function of SoC in comparable circuit models [20] or fractional order models [30]. Calculating the SoC is easy after the OCV is determined.

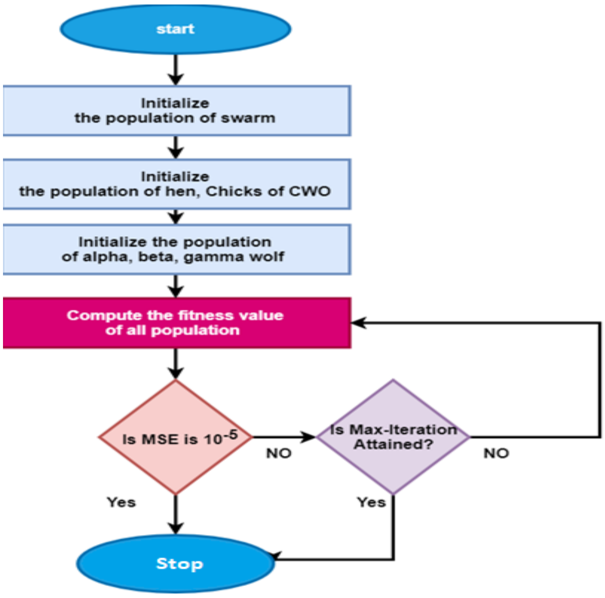

Fig. 2: Flow diagram of the proposed hybrid CWO-GWO algorithm

Proposed forecasting Method

Single-stage forecasting can be used for a specific period, but it cannot be used for multi-time-scale prediction. Furthermore, sharing data at multiple time scales is valid on an excellent forecasting resource.

These are the primary reasons for proposing a new technique for performing multi-time scale anticipating models. EV battery forecasting models use available data to predict SoC across a range of time scales. Because data used for short-term forecasting cannot be used for long-term forecasting, the duration of each task is determined by the availability of battery output data. It is possible to meet several forecasting needs in this chapter using hourly irradiance data; however, due to a lack of data, this cannot be done in a single-stage model.

Proposed hybrid CSO-GWO optimization algorithm

The absence of a more optimal compromise between the algorithm's exploratory and exploitative capabilities is the main challenge for swarm intelligence systems. The population's capacity for a worldwide search is defined by the exploration ability, which is the prey identification process of an individual within the population. Once the quarry is located, the exploitation capability allows the whole populace to work together to feast. Premature convergence, delayed convergence, local stagnation, local optimum and global optimal entrapment, etc. are all problems plaguing population-based algorithms.

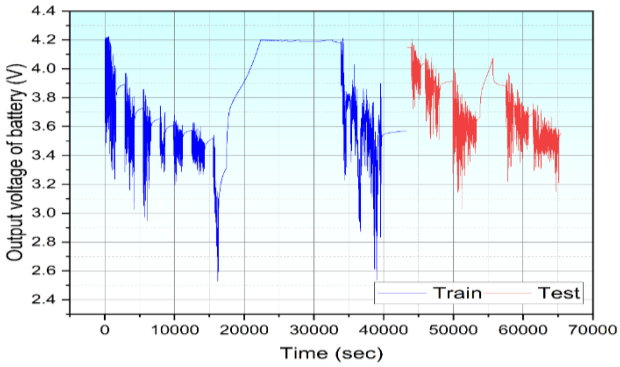

Fig. 3: Output voltage of the battery train and test data

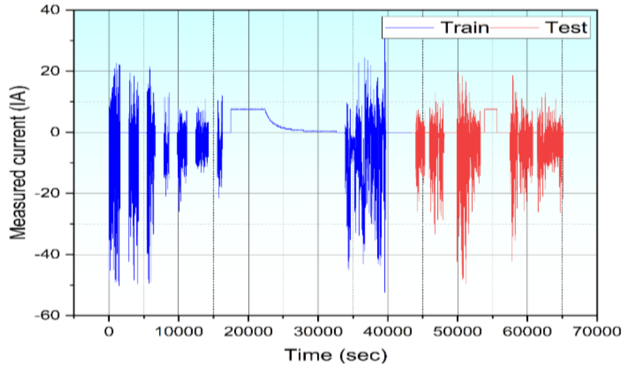

Fig. 4: Measured current of the battery train and test data

Two algorithms are combined in the suggested model to deal with these complications: the CWO optimizer, which excels at exploration, and the GWO, which excels in local hunting. Additionally, there is a social behaviour parallel between the two algorithms in the form of a three-tiered hierarchy.

RESULTS AND DISCUSSION

The most important operational characteristic of an electric vehicle is its estimated battery state of charge. The steps involved in the battery analysis are depicted in Figs. 3 and 4. The data was provided by McMaster University in Hamilton, Ontario, Canada. The characteristics of the battery, such as voltage, current, and temperature, are used to select the features. A standardised set of battery voltages, currents, and temperatures results from reduced variability during training and a faster training procedure. The research in this study considers the speed characteristics of electric vehicles. An emission cycle based on UDDS, a LA92 cycle, and SFTP are being used as part of the investigation into the accuracy of the proposed method for estimating SoC. To forecast

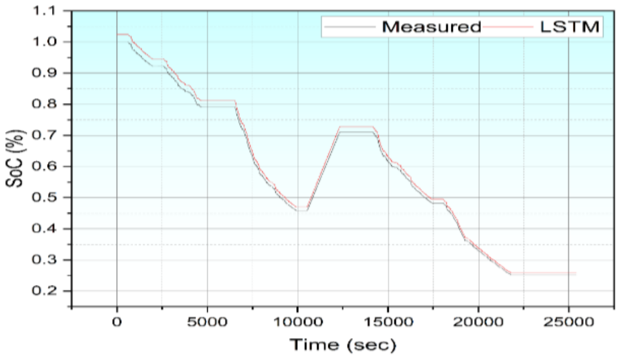

Fig. 5: LSTM and Measured SoC Prediction

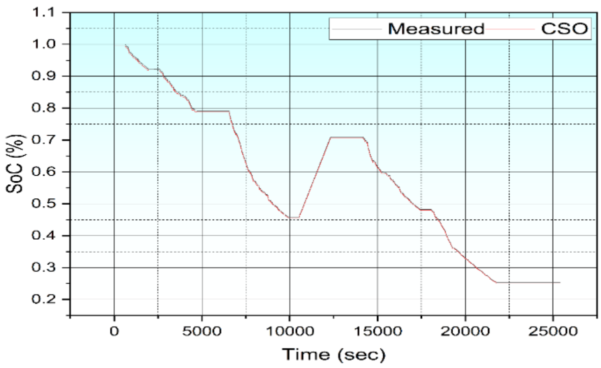

Fig. 6: CSO-LSTM and Measured SoC Prediction

the battery SoC, algorithms such as LSTM and hybrid LSTM CSO-GWO are used.

In the study, three approaches are used to assess the accuracy of SOC estimations: CSO, GWO, and a hybrid CSO-GWO LSTM. It is worth noting that the new FF-RLS technique is used to identify all of the battery properties that are used to estimate SOC. To begin, the test battery is fully charged using the CC-CV charging method. When the terminal voltage reaches 2.75 V, the current profiles recorded with the Urban Dynamometer Driving Schedule (UDDS) are applied repeatedly. Figs. 3 and 4 show the test and training data for voltage and current.

The most important operational characteristic of an electric vehicle is the estimated battery state of charge. The steps involved in the battery's analysis are depicted in Figs. 3 and 4. The data was supplied by McMaster University in Hamilton, Ontario, Canada. The features are chosen based on battery characteristics such as voltage, current, and temperature. A standardised set of battery voltages, currents, and temperatures is produced as a result of reduced variability during training and a faster training procedure. The speed characteristics of electric vehicles are considered in this study's research. An emission cycle based on UDDS, a LA92 cycle, and SFTP is being used as part of the investigation into the accuracy of the proposed method for estimating SoC. To forecast the battery SoC, algorithms like LSTM and hybrid LSTM CSO-GWO are used.

Three approaches are used in the study to assess the accuracy of SOC estimations: CSO, GWO, and a hybrid CSO-GWO LSTM. It is worth noting that the new FF-RLS technique is used to identify all of the battery properties that contribute to SOC estimation. To begin, the CC-CV charging method is used to fully charge the test battery. When the terminal voltage falls below 2.75 V, the current profiles recorded with the urban dynamometer driving schedule (UDDS) are applied repeatedly. Figs. 3 and 4 show the voltage and current test and training data.

The most accurate of these four filters is the AHIF. Rather than making assumptions about the statistical properties of noise, as required by Kalman filters, the AHIF suppresses interference norms into a defined range, allowing observers to solve constrained signals and significantly increasing their resilience. Accurate estimation provides reliable basic knowledge for SOC singularity analysis. If the RMSE, maximum absolute error, and mean absolute error are all less than 1%, a singularity can be avoided. Table 2 compares the SOC estimate errors based on various models to validate the efficacy of our proposed strategy. The maximum absolute error and Root Mean Square Error (RMSE) of the CSO algorithm are 5.6 percent and 2.57 percent, respectively, which are higher than those of the suggested technique. Furthermore, the proposed technique outperforms the reduced-order electrochemical model in terms of convergence time. The overall convergence time of a reduced-order electrochemical model using the A-SPKF algorithm is about one-fourth that of the proposed technique, but the electrochemical model takes 123 s to reach its reference value. Finally, the comparisons show that the proposed technique outperforms the majority of previously published electrochemical model-based methods.

Using the proposed fusion estimation approach, the proposed SOC estimating technique is tested on cells of varying ageing states. The test battery is charged using the CC-CV charging technique until the terminal voltage drops to 2.75 volts at room temperature. The first step in determining the battery's SOH is to extract the unique characteristics of the charging process. When the battery

Table 2: Performance metrics of battery at various drive cycles

Drive cycles	Algorithm	MSE	RMSE	NRMSE	MAE	MAPE	R^2
	CSO	0.0298	0.156	0.22127	0.013	0.00018	0.9945
UDDS	GWO	0.0245	0.145	0.214	0.012	0.00014	0.956
	CSO-GWO	0.021	0.125	0.2065	0.011	0.00012	0.945
	CSO	0.0157	0.1154	0.1724	0.00323	0.00019	0.9978
LA92	GWO	0.6125	0.2325	0.424	0.01421	0.00071	0.965
	CSO-GWO	0.0100	0.100	0.142	0.00221	0.00009	0.9425
	CSO	0.02256	0.1354	0.1984	0.0154	0.00050	0.99410
US06	GWO	0.04586	0.2154	0.3054	0.04632	0.00225	0.954
	CSO-GWO	0.00302	0.05234	0.08754	0.00325	0.00018	0.9932

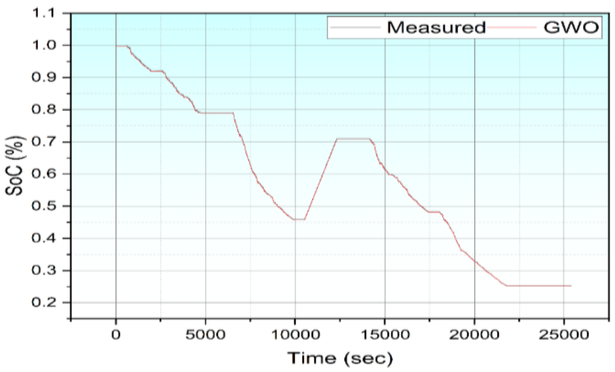

Fig. 7: GWO-LSTM and Measured SoC Prediction

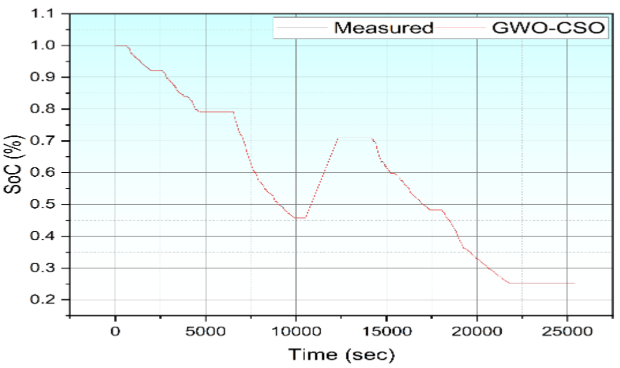

Fig. 8: hybrid GWO-CSO-LSTM and Measured SoC Prediction

runs out of power, the updated capacity is used to calculate the SOC. In this scenario, SOC is set at 20% for all aged cells, and the difference is clearly 80 percent. The SOC estimate findings for aged cells are shown in Fig. 8 and Table 2. To keep things simple, we'll just talk about four levels of old age: 97 percent alive, 93 percent alive, 88 percent alive, and 85 percent alive. As can be seen, the total discharge time decreases with time as the battery ages under the same conditions. The algorithm's ability to handle ageing cells has been demonstrated by its ability to generate accurate SOC estimates across a range of ageing states. For four distinct SOH statuses, there is a 60-30% SOC estimation error; this is the largest range of SOC estimation error. As illustrated in Fig. In this range, the relationship between SOC and OCV is very flat (c). Under these conditions, the suggested technique's SOC estimate error is limited to 1.2 percent. The final battery characteristics shown in Fig. 1 are OCV, ohmic resistance, polarisation resistance, and time constant. 8(c)- (f). The OCV curves show a noticeable variation as the battery ages. When the SOC drops from 60% to 4%, the OCV drops by 0.016 V, resulting in a 1.4 percent error in the SOC estimate. However, the battery's properties change noticeably as it ages. The ohmic resistance in the intermediate SOC area is very small and develops slowly, whereas the ohmic resistance in the lower SOC area rises quickly and is usually greater than the ohmic resistance in the higher SOC area. Globally, as SOH decreases, the ohmic resistance increases. The same is true of resistive polarisation. This means that, as the ageing process progresses, a real-time update of battery properties is required to improve SOC computation. Based on these comparisons, it is clear that the proposed SOC estimation technique works well across a wide range of life cycles. Fig. 9 depicts the various algorithms' performance metrics. The working conditions of UDDS, LA92, and SFTP, which indicate the real consumption of power batteries, can be used to validate SoC battery estimations. Under UDDS, LA92, and SFTP, the automobile must also accelerate or split. Fig. 2 depicts the normalised battery voltage input feature. The variation in battery current is depicted in Fig. 3. If the current rate is out of control, limit values should be used. During testing, the current sensor and voltmeter can measure the current and voltage

Table 3: globally reported feature selection of the SoC prediction

Feature Parameter	Battery	Performance index & Precision		Reference
(current, voltage)	NASA 18650	MAE	<1.29%	[31]
Temperature	NASA 18650	RMSE	<3.58%	[32]
charging voltage curve	NASA 18650	RMSE	<3.45%	[33]
discharging voltage curve	NASA 18650	RMSE	<3.84%	[34]
charging curve	NCM/ graphite	RMSE	2%	[35]
discharging curve	NASA 18650	MAE	<1.29%	[36]
peak, valley	Prismatic Li-ion Battery	RMSE	2.99%	[37]
(current, voltage)	NASA 18650	RMSE	<1.1%	Present study

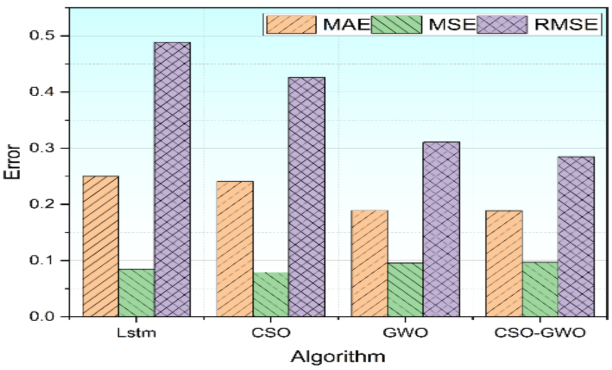

Fig. 9: performance metrics of the Hybrid, CSO, GWO LSTM of the optimization algorithm

of the battery cells in real time. It is connected to a thermocouple, which sends temperature data to a test system on the battery module. The test assumes that the lithium battery in the electric vehicle is charged in a stationary environment and operates at varying ambient temperatures throughout the experiment. The battery is now being charged at a rate of 15.5 amps per volt for a total of 15.5 amps (4.2 V). Fig. 4 depicts the standard lithium battery cell testing temperatures of 0, 10, and 25 °C, which are consistent with the previously discussed 0 to 25 °C temperature range. The battery module testing equipment is used to compute SoC reference values. The surface temperatures of the first battery cell are nearly identical when the ambient temperature is 25 degrees Celsius.

The temperature of the battery rises differently during a high-current-rate discharge. Temperature and temperature change are not synonymous. Because UDDS, LA92, and SFTP all operate in a single operational state, the battery temperature does not change significantly. As the SoC level is reduced, battery temperatures rise.

Fig. 5 depicts the SoC estimates of the impacts of UDDs, LA92, and SFTP on Algorithms LSTM and CSO at 0°C operating temperatures. Table 2 also includes the selection and specification of MAE, RMSE, and SD for SoC estimate error analysis. Estimated SoC results from multiple techniques work quite well at 0°C. If the temperature is not taken into account when using UDDS mode, SoC estimate errors increase over time. The SoC calculation results show an apparent 0°C difference [38-44].

The battery discharge characteristics change the LSTM assessment technique findings by a small margin at low temperatures. SoC estimation during the LA 92-error can be easily maintained and kept to zero degrees Celsius if the suggested combination approach is used. The LSTM estimator has a SoC error of 3%, which is consistent with the previous estimate. The GWO method's error rate increases over time in the SFTP drive loop. The estimator will be able to better monitor the true SoC value using this estimating strategy. The LSTM estimator also provides a wide range of errors that are within the acceptable range [45-50]. Table 3 compares the previously reported literature with the respective algorithm.

CONCLUSIONS

This study examines battery deterioration and dynamic operating temperatures using an adaptive fusion approach. An improved online identification technique based on an improved recursive least square method with the forgetting factor can identify model parameters over a wide temperature range. The battery's state of charge can be more accurately assessed using the least squares support vector machine approach. We can estimate that the error is less than 2% as a result of the tests. To analyse the charge status, the adaptive H-infinity filter is presented, which is based on a constantly updated state of health and an accurate battery model. Although all three of these algorithms are widely used, the one we developed outperforms them in terms of accuracy, speed, and sensitivity to environmental factors such as temperature shifts and battery deterioration. Following a thorough investigation, the method was discovered to have a wide range of applications in the evaluation of lithium-ion battery state-of-charge and health. It is also possible that the proposed method will aid in predicting the state of affairs of the charge singularity. As battery management systems improve at predicting the state of charge, the residual state of charge threshold for singularity prediction accuracy may be reduced. The relationship between charge state evaluation and singularity prediction will be investigated further. The method will be evaluated in electric vehicle battery packs on a printed circuit board controller to validate the design's battery management system estimation performance. Additional research is required to determine how to deal with temperature and capacity discrepancies across cells in a pack and provide an official estimate.

Received : Aug. 21, 2022 ; Accepted : Dec, 19, 2022

REFERENCES

[1]Chandran V., Patil C.K., Karthick A., Ganeshaperumal D., Rahim R., Ghosh A., State of Charge Estimation of Lithium - Ion Battery for Electric Vehicles Using Machine Learning Algorithms, *World Electric Vehicle Journal*, **12**: 38 (2021).

[2] How D.N.T., Hannan M.A., Hossain Lipu M.S., Ker P.J., State of Charge Estimation for Lithium-Ion Batteries Using Model-Based and Data-Driven Methods: A Review, *IEEE Access*, **7**: 136116–136136 (2019).

[3] Vellingiri M.T., Mehedi I.M., Palaniswamy T., A Novel Deep Learning-Based State-of-Charge Estimation for Renewable Energy Management System in Hybrid Electric Vehicles, *Mathematics*, **10**: 260 (2022).

[4] Kabilan R., Chandran V., Yogapriya J., Karthick A., Gandhi P.P., Mohanavel V., Rahim R., Manoharan S., Short-Term Power Prediction of Building Integrated Photovoltaic (BIPV) System Based on Machine Learning Algorithms, *International Journal of Photoenergy* (2021).

[5] Wei Z., Zou C., Leng F., Soong B.H., Tseng K.J., Online Model Identification and State-of-Charge Estimate for Lithium-Ion Battery with a Recursive Total Least Squares-Based Observer, *IEEE Transactions on Industrial Electronics*, **65**: 1336–1346 (2018).

[6] Shamsipur M., Bahrami Adeh N., Hajitarverdi M.S., Yazdimamagan M., Zarei F., Influence of Micro Silica a Mechanical Properties of Plasticized Sulur Composites, *Iran. J. Chem. Chem. Eng. (IJCCE)*, **32(3)**:1-7 (2013).

[7] Coleman M., Lee C.K., Zhu C., Hurley W.G., State-of-Charge Determination from EMF Voltage Estimation: Using Impedance, Terminal Voltage, and Current for Lead-Acid and Lithium-Ion Batteries, *IEEE Transactions on Industrial Electronics*, **54**: 2550–2557 (2007).

[8] Srivastav S., Lacey M.J., Brandell D., State-of-Charge Indication in Li-Ion Batteries by Simulated Impedance Spectroscopy, *Journal of Applied Electrochemistry*, **47**: 229–236 (2017).

[9] Tong S., Lacap J.H., Park J.W., Battery State of Charge Estimation Using a Load-Classifying Neural Network, *Journal of Energy Storage*, **7**: 236–243 (2016).

[10] Bi J.; Wang Y.; Shao S.; Cheng Y. Residual Range Estimation for Battery Electric Vehicle Based on Radial Basis Function Neural Network, *Measurement: Journal of the International Measurement Confederation*, **128**: 197–203 (2018).

[11] Xu Z., Wang J., Fan Q., Lund P.D., Hong J., Improving the State of Charge Estimation of Reused Lithium-Ion Batteries by Abating Hysteresis Using Machine Learning Technique, *Journal of Energy Storage*, **32**: *(*2020).

[12] Singh P., Vinjamuri R., Wang X., Reisner D., Design and Implementation of a Fuzzy Logic-Based State-of-Charge Meter for Li-Ion Batteries Used in Portable Defibrillators, *Journal of Power Sources*, **162**: 829–836 (2006).

[13] Lai X., Qiao D., Zheng Y., Zhou L., A Fuzzy State-of-Charge Estimation Algorithm Combining Ampere-Hour and an Extended Kalman Filter for Li-Ion Batteries Based on Multi-Model Global Identification, *Applied Sciences (Switzerland)* **8**: (2018).

[14] Dai H., Zhang X., Wei X., Sun Z., Wang J., Hu F., Cell-BMS Validation with a Hardware-in-the-Loop Simulation of Lithium-Ion Battery Cells for Electric Vehicles, *International Journal of Electrical Power and Energy Systems*, **52**: 174–184 (2013).

[15] Hua Y., Cordoba-Arenas A., Warner N., Rizzoni G., A Multi Time-Scale State-of-Charge and State-of-Health Estimation Framework Using Nonlinear Predictive Filter for Lithium-Ion Battery Pack with Passive Balance Control, *Journal of Power Sources*, ***280***: 293–312 (2015).

[16] Feng F., Hu X., Hu L., Hu F., Li Y., Zhang L., Propagation Mechanisms and Diagnosis of Parameter Inconsistency within Li-Ion Battery Packs, *Renewable and Sustainable Energy Reviews*, **112**: 102–113 (2019).

[17] Xiong R., Sun F., Gong X., He H., Adaptive State of Charge Estimator for Lithium-Ion Cells Series Battery Pack in Electric Vehicles, *Journal of Power Sources*, **242**: 699–713 (2013).

[18] Sun F., Xiong R., A Novel Dual-Scale Cell State-of-Charge Estimation Approach for Series-Connected Battery Pack Used in Electric Vehicles, *Journal of Power Sources*, **274**: 582–594 (2015).

[19] Sun F., Xiong R., He H., A Systematic State-of-Charge Estimation Framework for Multi-Cell Battery Pack in Electric Vehicles Using Bias Correction Technique, *Applied Energy*, **162**:1399–1409 (2016).

[20] Zhong L., Zhang, C., He, Y. Chen, Z. A Method for the Estimation of the Battery Pack State of Charge Based on In-Pack Cells Uniformity Analysis. *Applied Energy*, ***113***: 558–564 (2014).

[21] Chen Z., Li X., Shen, J., Yan W., Xiao R., A Novel State of Charge Estimation Algorithm for Lithium-Ion Battery Packs of Electric Vehicles. *Energies (Basel)*, **9**: (2016).

[22] Deng Z., Hu X., Lin X., Che Y., Xu L., Guo W., Data-Driven State of Charge Estimation for Lithium-Ion Battery Packs Based on Gaussian Process Regression, *Energy*, **205**: (2020).

[23] Lin X., Real-Time Prediction of Anode Potential in Li-Ion Batteries Using Long Short-Term Neural Networks for Lithium Plating Prevention, *Journal of the Electrochemical Society*, **166**: A1893–A1904 (2019).

[24] Hamar J.C., Erhard S., v., Zoerr C., Jossen A., Anode Potential Estimation in Lithium-Ion Batteries Using Data-Driven Models for Online Applications, *Journal of the Electrochemical Society*, **168**: 030535 (2021).

[25] Bonfitto A., Ezemobi E., Amati N., Feraco S., Tonoli A., Hegde S., "State of Health Estimation of Lithium Batteries for Automotive Applications with Artificial Neural Networks", *AEIT International Conference of Electrical and Electronic Technologies for Automotive, AEIT AUTOMOTIVE 2019*, 1–5 (*2019).*

[26] Ling L., Wei Y., State-of-Charge and State-of-Health Estimation for Lithium-Ion Batteries Based on Dual Fractional-Order Extended Kalman Filter and Online Parameter Identification, *IEEE Access*, **9**: 47588–47602 (2021).

[27] Remmlinger J., Buchholz M., Meiler M., Bernreuter P., Dietmayer K., State-of-Health Monitoring of Lithium-Ion Batteries in Electric Vehicles by on-Board Internal Resistance Estimation , *Journal of Power Sources*, **196**: 5357–5363 (2011).

[28] Jin G., Li L., Xu Y., Hu M., Fu C., Qin D., Comparison of SOC Estimation between the Integer-Order Model and Fractional-Order Model under Different Operating Conditions, *Energies (Basel)*, **13**: (2020).

[29] Liu B., Liu S., Guo S., Zhang S., Economic Study of a Large-Scale Renewable Hydrogen Application Utilizing Surplus Renewable Energy and Natural Gas Pipeline Transportation in China, *International Journal of Hydrogen Energy*, **45**: 1385–1398 (2020).

[30] Waag W., Fleischer C., Sauer D.U., Adaptive On-Line Prediction of the Available Power of Lithium-Ion Batteries, *Journal of Power Sources*, **242**: 548–559 (2013).

[31] Li Y., Sheng H., Cheng Y., Stroe D.I., Teodorescu, R. State-of-Health Estimation of Lithium-Ion Batteries Based on Semi-Supervised Transfer Component Analysis, *Applied Energy*, **277**: (2020).

[32] Mawonou K.S.R., Eddahech A., Dumur D., Beauvois D., Godoy E., State-of-Health Estimators Coupled to a Random Forest Approach for Lithium-Ion Battery Aging Factor Ranking, *Journal of Power Sources*, (2020).

[33] D., Zhang X., Pan R., Wang Y., Chen Z., A Novel Gaussian Process Regression Model for State-of-Health Estimation of Lithium-Ion Battery Using Charging Curve, *Journal of Power Sources*, **384**: 387–395 (2018).

[34] Lu C., Tao L., Fan H., Li-Ion Battery Capacity Estimation: A Geometrical Approach, *Journal of Power Sources*, **261**: 141–147 (2014).

[35] Shu X., Li G., Zhang Y., Shen J., Chen Z., Liu Y., Online Diagnosis of State of Health for Lithium-Ion Batteries Based on Short-Term Charging Profiles, *Journal of Power Sources*, **47**: (2020).

[36] Li W., Jiao Z., Du L., Fan W., Zhu Y., An Indirect RUL Prognosis for Lithium-Ion Battery under Vibration Stress Using Elman Neural Network, *International Journal of Hydrogen Energy*, **44**: 12270–12276 (2019).

[37] Stroe D.I., Schaltz E., Lithium-Ion Battery State-of-Health Estimation Using the Incremental Capacity Analysis Technique, *IEEE Transactions on Industry Applications*, **56**: 678–685 (2020).

[38] Babapoor A., Azizi M.M., Karimi G., Thermal Management of a Li-ion Battery Using Carbon Fiber-PCM Composites, *Applied Thermal Engineering*, **82(c)**: 281–290 (2015).

[39] Babapoor] A., Karimi G., Thermal Properties Measurement and Heat Storage Analysis of Paraffin-Nanoparticles composites phase change material: comparison and optimization ,*Applied Thermal Engineering*, **90:** 945-951 (2015).

[40] Samimi F., Babapoor A., Azizi M.M, Karimi G., Thermal Management Analysis of a Li-Ion Battery Cell Using Phase Change Material Loaded with Carbon Fibers, *Energy* , **96**: 355-371 (2016).

[41] Babapoor A., Karimi G., Khorram M., Fabrication and Characterization of Nanofiber-Nanoparticle-Composites with Phase Change Materials by Electrospinning, *Applied Thermal Engineering*, **99**:1225-1235 (2016).

[42] Babapoor A., Karimi G., Sabbaghi S., Thermal CHaracteristic of Nanocomposite Phase Change Materials During Solidification Process, *Journal of Energy Storage*, **7**: 74-81 (2016).

[43] Karimi G., Azizi M.M., Babapoor A., Experimental Study of a Cylindrical Lithium Ion Battery Thermal Management Using Phase Change Material Composites, *Journal of Energy Storage*, **8**:168–174 (2016).

[44] Babapoor A., Karimi G., Golestaneh S.I., Ahmadi Mezjin M., Coaxial Electro-Spun PEG/PA6 Composite Fibers: Fabrication and Characterization, *Applied Thermal Engineering*, **118**: 398-407 (2017).

[45] Golestaneh S.I., Karimi G., Babapoor A., Torabi F., Thermal Performance of Co-Electrospun Fatty Acid Nanofiber Composites in the Presence of Nanoparticles, *Applied Energy*, **212**: 552-564 (2018).

[46] Sakkaki M., Moghanlou F.S., Parvizi S., Baghbanijavid H., Babapoor., Shahedi Asl M., Phase Change Materials as Quenching Media for Heat Treatment of 42CrMo4 Steels, September (2019).

[47] Haghighi A., Babapoor A., Azizi M.M., Javanshir Z., Ghasemzadeh H., Optimization of the Thermal Performance of PCM Nanocomposites, *Journal of Energy Management and Technology (JEMT)* (2019).

[48] Najafi B., Bahari M., Babapoor A., Evaluation of α-AL_2O_3-PW Nanocomposites for Thermal Energy Storage in the Agro-Products Solar Dryer, *Journal of Energy Storage*, **28**: 101181 (2020).

[49] Babapoor A., Haghighi A., Jokar S.M., Ahmadi Mezjin M., The Performance Enhancement of Paraffin as a PCM During the Solidification Process: Utilization of Graphene and Metal Oxide Nanoparticles, *Iran. J. Chem. Chem. Eng. (IJCCE),* **41(1):** 37-48 (2022).

[50] Ahmadi Mezjin M., Karimi G., Medi B., Babapoor A., Paar M., Passive Thermal Management of a Lithium-Ion Battery Using Carbon Fiber Loaded Phase Change Material: Comparison and Optimization, *Iran. J. Chem. Chem. Eng. (IJCCE),* **41(1):** 310-327 (2022).